Bioresource Technology 253 (2018) 33–40

Contents lists available at ScienceDirect

Bioresource Technology

journal homepage: www.elsevier.com/locate/biortech

Effective algal harvesting by using mesh membrane for enhanced energy recovery in an innovative integrated photobioelectrochemical system

Shuai Luo, Pranav Sai Shankar Sampara, Zhen He*

Department of Civil and Environmental Engineering, Virginia Polytechnic Institute and State University, Blacksburg, VA 24061, USA

GRAPHICAL ABSTRACT

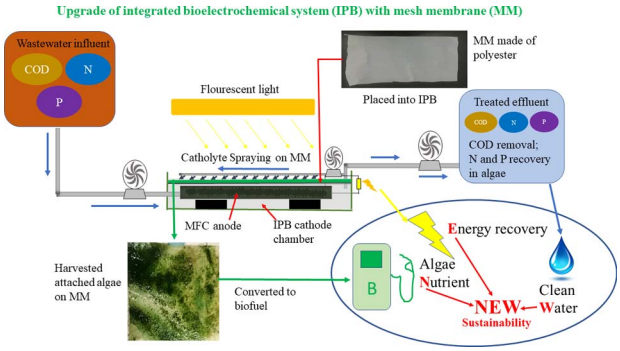

ARTICLE INFO

Keywords:
Integrated photobioelectrochemical system
Algae harvesting
Mesh membrane
Energy recovery
Wastewater treatment

ABSTRACT

In this work, an innovative design of integrated photobioelectrochemcial system (IPB) and an algal harvesting method based on polyester-mesh membrane (MM) were investigated. The algal growth/harvesting period of 6 days led to the highest surface biomass productivity (SBP) of 0.88 g m^{-2} day^{-1} and the highest energy generation of 0.157 ± 0.001 kJ day^{-1}. The harvesting frequency of 3 times in an operational cycle (with three pieces of MM) enhanced the SBP to 1.14 g m^{-2} day^{-1}. The catholyte recirculation for catholyte mixing resulted in a positive net energy production (NEP) of 0.227 ± 0.025 kJ day^{-1}. Those results have demonstrated the benefits of both using mesh membrane and the new reactor design for algal collection with positive effects on improving IPB performance.

1. Introduction

It has been well recognized that wastewater treatment consumes a significant amount of energy (Henze, 2002), for example about 2–3% of the electrical energy in the U.S. (McCarty et al., 2011). Sustainable wastewater treatment favors recovery of useful resources such as energy and value-added products with simultaneous waste reduction. The energy potential in the dissolved organics in a municipal wastewater is about 4 kWh kg^{-1} $COD_{removed}$ (Escapa et al., 2014), and recovery of this energy will help offset energy consumption by the treatment process. Energy can be recovered in the form of biogas, bioelectricity, and/or biomass via different treatment methods. In addition to energy recovery, reducing energy consumption will also play a key role in achieving energy-neural or even positive wastewater treatment. Because the major energy consumption (> 50%) in the existing domestic wastewater treatment is due to aeration (Wei et al., 2003), development of anaerobic-based treatment or alternative approaches for providing dissolved oxygen will be of great interest.

* Corresponding author.
E-mail address: zhenhe@vt.edu (Z. He).

https://doi.org/10.1016/j.biortech.2018.01.001
Received 28 November 2017; Received in revised form 29 December 2017; Accepted 1 January 2018
Available online 03 January 2018
0960-8524/

As an emerging treatment concept, integrated photo-bioelectrochemical systems (IPB) link microbial fuel cells (MFCs) with algal growth to accomplish low energy consumption (via anaerobic treatment and elimination of external aeration) and energy recovery (both bioelectricity and algal biomass) (Luo et al., 2017a; Xiao and He, 2014). An IPB system can take advantage of MFCs to use electrogenic bacteria to simultaneously degrade organic compounds and generate electricity by oxygen reduction reaction (Xiao et al., 2012). The oxygen reduction reaction occurs on the cathode like regular MFCs to complete the electrical circuit between the anode and the cathode (Logan et al., 2006). In the presence of algae, oxygen is supplied to the cathode via photosynthesis, instead of external aeration, and the anode effluent flows into the cathode compartment as a catholyte for nutrient removal (e.g., N, P) by algae, thereby eliminating the need for aeration and resulting in lower energy consumption (Xiao et al., 2012). In addition, algal biomass can be potentially harvested for production of biofuel or other value-added products such as bioplastic (Mata et al., 2010). Bioelectricity generation in an IPB system is relatively straightforward and can be harvested by using power management system (Wang et al., 2015). Algal biomass, on the other hand, will need much effort to achieve effective collection. Algal biomass could yield 30–50% weight to produce oil for biodiesel production, which has an energy density of ~41 MJ kg^{-1} (Demirbas and Fatih Demirbas, 2011). Many algal species prefer to form biofilm on a solid surface (Gross et al., 2015; Kesaano and Sims, 2014; Liu et al., 2013), which is usually the cathode electrode of an IPB. The reported methods for algal harvesting from IPB involve manual scraping and filtration of the catholyte (Hou et al., 2016; Ma et al., 2017). Manual collection of algal biomass in the cathode requires the MFC to be removed out of the cathode compartment and this would create significant challenges for a practical system. Filtration of the catholyte can only harvest the suspended biomass, and the attached biomass must require manual detachment into the liquid phase, which would be difficult in a large-scale system. Therefore, new harvesting methods will be needed for convenient and effective algal collection from IPB systems.

To minimize the effect of algal biomass harvesting on the cathode, separating algal growth from the IPB cathode may be considered but algae should still be adjacent the cathode electrode for providing dissolved oxygen and taking up nutrients. Mesh membrane (MM) has been used to harvest algal biomass and may be installed in an IPB to facilitate algal collection. Various types of MM have been examined for their capability of algal attachment, material durability, and cost effectiveness. It was reported that cotton duct could serve as an effective carrier for the algal attachment in a rotating algal biofilm cultivation system (Gross et al., 2013). The stainless steel woven mesh with a membrane pore size of 5 μm was shown to achieve excellent production of algal biomass (Zhang et al., 2014). Different lignocellulosic materials including pine sawdust and rice husk have also been investigated as carriers for the algal attachment with reducing the operational cost for algal harvesting (Zhang et al., 2017). Synthetic materials such as nylon and polyester were found to have suitable surface texture and physicochemical properties to obtain the satisfactory biomass productivity (Gross et al., 2016). Other materials that were studied for algal growth and attachment included the glass fiber, plain printing paper, filter paper, and cellulose acetate membrane (Liu et al., 2013; Shi et al., 2014). Those prior efforts indicate a good potential of using MM to collect algal biomass, for example in an IPB system, but this has not been investigated before.

The goal of this study was to design a configuration for IPB that could facilitate algal collection and to formulate a strategy for effective algal biomass harvesting using MM. Two MM materials, made of nylon and polyester of various pore sizes, were initially examined for algal growth and harvesting in an IPB. The polyester-MM was selected for further experiments to understand the effects of algal growth/harvesting periods and harvesting frequencies on biomass collection and energy production. Finally, catholyte recirculation, a method for catholyte mixing, was studied and compared to mechanical mixing and constant aeration for overall energy performance.

2. Materials and methods

2.1. Mesh membrane material selection

In the algal attachment affinity test, six types of MMs made of polyester or nylon with different pore sizes (polyester at 0.11, 0.53 and 4.98 mm, and nylon at 0.11, 0.53 and 5.31 mm) were divided into three experimental groups (Supplementary Table S1). Two different MM materials with similar pore size (and the same physical size of 15 × 15.2 cm/each) were simultaneously installed in a water tank (15.2 × 30.5 × 20.3 cm) for side-by-side comparison (Supplementary Fig. S1). Illumination was provided by a light at 12 h on/12 h off. The water tank was filled with 6 L algal solution, consisting of deionized water supplemented with chemicals to mimic domestic wastewater according to a previous study (Luo et al., 2017b), and algae inocula (sampled from Duck Pond on Virginia Tech campus, Blacksburg, VA) to achieve an initial algal concentration of 1 g L^{-1}. Each test lasted for four cycles with a four-day period of each cycle to ensure sufficient algal attachment (Kakarla and Min, 2014), though the four-day period was not necessarily an optimal period to achieve the best algal growth. The weight of the harvested biomass in last three cycles (2–4 cycle) was used for comparison of algal attachment. Two polyester MM materials (0.11 and 0.53 mm) were further studied with eight-cycle cultivation to determine the better pore size for the following IPB experiments (Supplementary Table S1).

2.2. Integrated photobioelectrochemical system setup and operation

An IPB system was composed of two tubular MFCs (hydraulically connected in series and installed in the same water tank as that of the MM selection test) (Fig. 1). Each tubular MFC was made of cation exchange membrane (CEM, Ultrex CMI7000, Membranes International, Inc., Glen Rock, NJ) to separate the anode and the cathode compartments, with an anode working volume of 200 mL (diameter: 4.4 cm; length: 15 cm). The water tank functioned as both the algal bioreactor and the cathode compartment for the IPB with a liquid volume of 3 L. The anode electrode material was carbon brush, while the cathode electrode was carbon cloth coated with activated carbon (5 mg cm^{-2}) surrounding the CEM, prepared according to the previous work (Luo and He, 2016). Each tubular MFC was connected with one external resistor of 8.2 Ω to ensure relatively high current generation, and the total current was the sum of two MFCs.

Synthetic domestic wastewater was continuously pumped into the IPB anodes at a flow rate of 0.55 mL min^{-1}, resulting in an anodic hydraulic residence time (HRT) of 12 h. It contained (per L DI water): 0.35 g sodium acetate, 0.15 g NH_4Cl, 0.5 g NaCl, 0.015 g $MgSO_4$, 0.02 g $CaCl_2$, 0.6 g $NaHCO_3$, 0.027 g KH_2PO_4, and 1 mL trace element, resulting in a composition of ~270 mg L^{-1} COD, ~40 mg L^{-1} NH_4^+-N, and ~6 mg L^{-1} total phosphorus (TP). The anolyte effluent was discharged into the water tank as the catholyte, and the catholyte effluent was pumped out of the water tank at the same flow rate as the anolyte (the HRT in the cathode/algal bioreactor was 3.75 days). Two fluorescent bulbs (40 W, 125 V, 4100 K, GE, CT, USA) were installed on the top of the water tank, with light illumination at 12 h off/12 h. The catholyte mixing was initially provided by a stirring bar, which was in later experiment replaced by the catholyte recirculation.

2.3. Experiments

The experiments consisted of three groups for different purposes (Supplementary Table S2). Group 1 was to examine the time interval (4, 6 and 8 days) for algal growth/harvesting. Group 2 was to study the partial harvesting (or frequency) by collecting algal biomass formed on

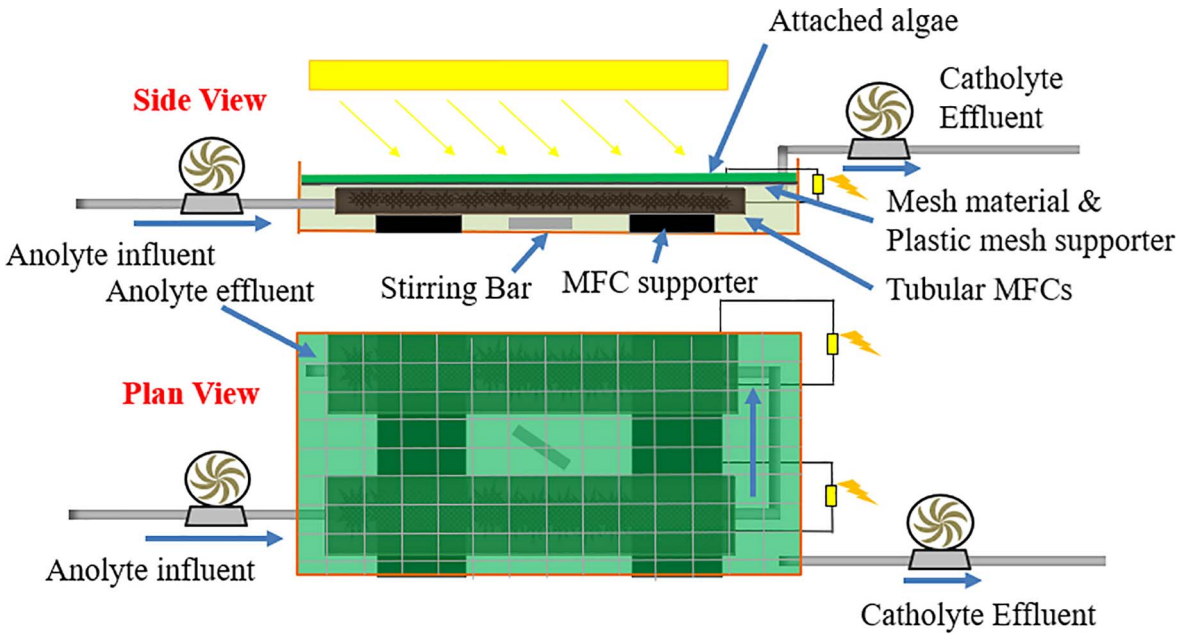

Fig. 1. Schematic of the IPB system containing mesh membrane for algal growth and harvesting and two tubular MFCs in serially hydraulic connection, using stirring to mix the catholyte.

a part of MM. To do this, three tests were performed with the same total surface area of MM: the first test was one piece of MM that was the same as that used in Group 1; the second test was two pieces of MM (each was ½ of the size of the total surface area); and the third test was three pieces of MM (each was 1/3 of the size of the total surface area). In the second and third tests, one (small) piece was removed for algal biomass collection, while the rest were remained in the reactor for future harvesting. The total harvesting time was 6 days in each test; that meant in the first test, the whole piece of MM would be removed for algal biomass collection every 6 days, while in the second and third tests, each (small) piece of MM was removed for algal harvesting every 3 or 2 days (in total, each IPB had 6 days for algal harvesting in each cycle). Group 3 (three pieces of MM in the IPB) was to investigate the method for catholyte mixing, including continuous aeration (50 mL min^{-1}, no algae), stirring (same as that in Groups 1 and 2), and catholyte recirculation. To perform catholyte recirculation, the stirring was removed and the catholyte was returned to the top of MM by a pump at 50 mL min^{-1} (Supplementary Fig. S2).

2.4. Measurement and calculations

For the MM material selection, the attached algae on the MMs were scraped off after one cycle and measured for weight. In the IPB experiment, the voltage of the IPB was recorded every 5 min by a digital multimeter (2700, Keithley Instruments, Inc., Cleveland, OH). The concentrations of soluble COD, NH_4^+-N, NO_3^--N, and TP were measured by using a DR/890 colorimeter (Hach Company, Loveland, CO, USA). The dissolved oxygen (DO) in the catholyte was measured by using a DO meter (Hanna Instrument, Woonsocket, RI, USA). The total Coulomb (TC) were calculated by integrating current over time in an operational cycle. The removal efficiencies (RE, %) of COD, NH_4^+-N and TP were also calculated. The algal biomass on the MM was scraped off and dried in a muffle oven for one day (50 °C) to obtain the dry weight, determined as harvested algal biomass (HAB, g). In contrast, non-harvested algal biomass (NHAB, g) was defined as the algal biomass attached on the wall of water tank and the cathode electrode of the MFCs, and suspended biomass in the catholyte.

Surface biomass productivity (SBP, g m^{-2} day^{-1}) was used to represent the algal growth rate on the MM (Gross et al., 2016), and determined as SBP = HAB/surface area of MM, which was 0.0392 m^2 in this study. Actual algal harvesting efficiency (AAHE, %) was calculated according to Eq. (1):

$$\mathrm{AAHE} = \frac{\mathrm{HAB}}{\mathrm{HAB} + \mathrm{NHAB}} * 100\% \quad (1)$$

where HAB represents the total HAB (g) from MM, and NHAB represents the total algal biomass (g) from other sources (e.g., wall surfaces of algal tank).

The total energy generation per day (EG, kJ day^{-1}) was estimated using Eq. (2), including both electricity generation (E_e, kJ day^{-1}) and harvested algal biomass (E_a, kJ day^{-1}):

$$\mathrm{EG} = \mathrm{E}_e + \mathrm{E}_a \quad (2)$$

The energy generation from algal biomass (E_a, kJ day^{-1}) was estimated according to Eq. (3):

$$E_a = \frac{\mathrm{HAB} * \eta_1 * \eta_2 * 3.78 * 10^4}{t} \quad (3)$$

where η_1 and η_2 represent the converting efficiency from harvested algal biomass to biodiesel (η_1 assumed as 0.4) and from the biodiesel to electricity (η_2 assumed as 0.3) (Tse et al., 2016; Xiao et al., 2012), respectively; the number " $3.78 * 10^4$ " represents the energy content (kJ) of harvested algal biomass per gram of HAB; and t represents the total time period (day) for each test (e.g., t = 18, 12 and 24 days for experimental group #1, Supplementary Table S2).

The energy consumption (EC) included the solution pumping, catholyte recirculation (in later experiment), stirring for catholyte mixing (in early experiment), and/or aeration (in the test that did not have algae). The energy consumption by the solution pumping (E_p, kJ day^{-1}) was calculated according to the following equation (Eq. (4)) (Zhang et al., 2013):

$$\mathrm{E}_p = (2 * Q_1 * E_1 + Q_2 * E_2) * \frac{86.4 * r}{6 * 10^7} \quad (4)$$

where Q_1 represents the flow rates of anolyte influent and catholyte effluent (Q_1 = 0.55 mL min^{-1}); Q_2 represents the flow rate of the catholyte recirculation rate effluent (Q_2 = 50 mL min^{-1}; Q_2 = 0 mL min^{-1} for experimental groups without catholyte recirculation); E_1 and E_2 represent the hydraulic pressure heads of two pumps (m) for the anolyte influent/catholyte effluent (E_1 = 0.016 m in this study) and the catholyte recirculation (E_2 = 0.025 m in this study), respectively; and r

is 9800 N m^{-3}. The energy consumption by the stirring (kJ day^{-1}) was assumed as 0.008 W with 400 rpm (0.69 kJ day^{-1}) according to the power consumption of turbine impeller in a 2 L stirring miniature bioreactor (Gill et al., 2008). The energy consumption of aeration was estimated as 160.7 kJ day^{-1} with the aeration rate at 50 mL min^{-1} (0.62 kWh m^{-3} air according to a previous reference (Qin et al., 2017)).

The net energy production (NEP, kJ day^{-1}) is the difference between energy generation and consumption. A negative NEP means that energy input is required, while a positive NEP indicates net energy output.

3. Results and discussion

3.1. Selection of optimal mesh membrane material

The selection of optimal MM material was performed by examining algal growth on two types of MM materials with three different pore sizes each (Supplementary Table S1). The results showed that the 1st cycle generally had very low SBP, because of the initiation for the algal attachment, and the 3rd and 4th cycles exhibited close results (Supplementary Fig. S3). This confirmed the previous findings that the SBP from the regrowth culture in later cycles would be higher than the initial growth (Christenson and Sims, 2012; Gross et al., 2016). Then, the MM comparison was based on the average SBPs from 2nd to 4th cycles. The MM made of polyester with a pore size of 0.11 mm and 0.53 mm had the higher SBPs (2.41 ± 0.41 and 2.82 ± 0.33 g m^{-2} day^{-1}, respectively) than that of other MMs ($p < .05$, two-tailed *t*-test) (Fig. 2), likely benefited from suitable surface texture of the polyester material for algal attachment (Gross et al., 2016; Su et al., 2016). However, the SBP comparison based on only 2–4 cycles was not sufficient to determine the pore size (0.11 mm and 0.53 mm) for the algal attachment, due to the possible cultivation instability in the initial cycles.

Next, a relatively long-term operation (8 cycles for 32 days, Supplementary Table S1) was performed to compare the MM made of polyester with two pore sizes, 0.11 and 0.53 mm, and the data from the last four cycles (5–8 cycles) were used for analysis. It was found that the SBP of the polyester with 0.53 mm had 4.13 ± 0.21 g m^{-2} day^{-1}, significantly higher than that with 0.11 mm (3.60 ± 0.27 g m^{-2} day^{-1}) (inset of Fig. 2, $p < .05$). This result was unexpected, because the attached algal attachment was supposed to increase with decreasing pore size that had better retention (Gross et al., 2016; Ozkan and Berberoglu, 2013). The surface texture of 0.53-mm MM might have helped with algal attachment, because that the single algal cells would easily accumulate to form the cluster with a much bigger size (possibly greater than 0.11 mm pore size MM in this study), which could make algae difficult to retain on the MM with a smaller pore size, but a very large pore size would also decrease algal attachment by allowing algal cells to pass through (Supplementary Fig. S3). This was supported by a previous study that showed the best algal attachment with 0.5-mm mesh openings (Gross et al., 2016). Therefore, the polyester MM with the pore size of 0.53 mm was chosen for the following experiments. It should be noted that the surface properties of the MM need to be studied by using techniques such as contact angle (hydrophobicity/hydrophilicity) and SEM/AFM (roughness), and chemical properties of the MM should be evaluated in order to determine any possible linkage of surface with algae. All of these will provide new directions in the research of IPB systems.

3.2. Effects of algal growth/harvesting period (Group 1)

Both the algal attachment and harvesting on the MM was strongly relevant to the algal growth the period before harvesting. Three growth/harvesting periods, 4, 6 and 8 days, were examined (Group 1, Supplementary Table S2). The growth/harvesting period changed DO and thus affected current generation (Fig. 3A and B). It was observed that the peak current increased from 1.50 mA on the 1st day to 3.68 mA at the end of 6th day for the growth/harvesting period of 6 days, with the peak DO concentration increasing from 2.80 (1st day) 5.91 mg L^{-1} (6th day). The increased DO concentration was a result of more algal accumulation on the MM and thus the increased oxygen production rate over time. The IPB with the 8-day growth/harvesting period had a total Coulomb production of 152.7 ± 36.1 C day^{-1}, significantly higher than that of the 4-day growth/harvesting period (92.5 ± 31.6 C day^{-1}) ($p < .05$), but not significantly different from that of the 6-day growth/harvesting period (121.3 ± 37.0 C day^{-1}) ($p > .05$). Regardless of the algal growth/harvesting periods, the IPB achieved comparable treatment performance, in terms of the removal

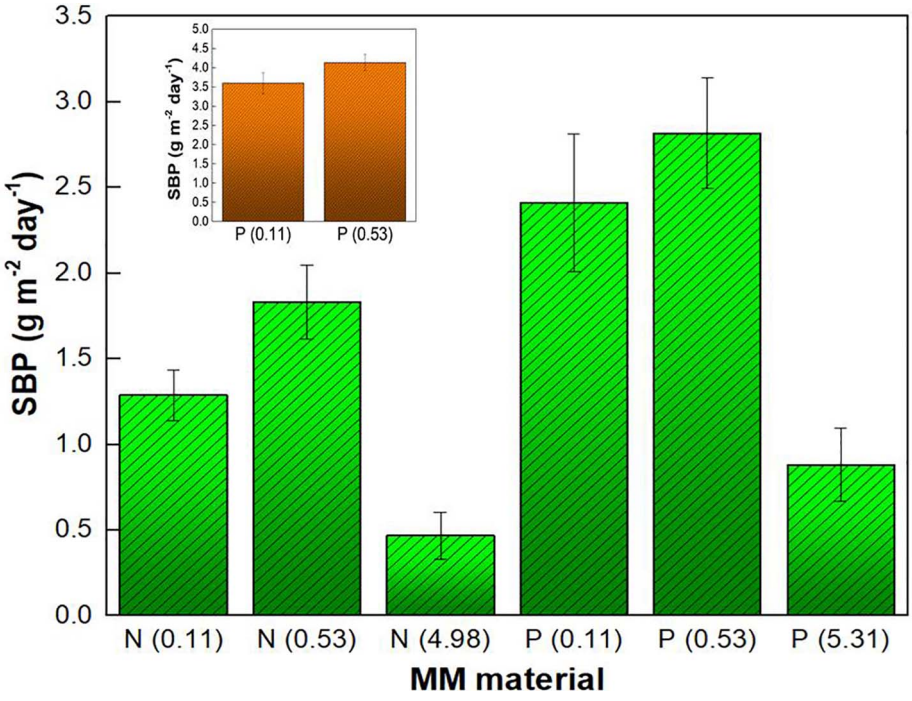

Fig. 2. Average surface biomass productivity (SBP, g m^{-2} day^{-1}) in three cycles (2–4 cycle) for two different MM materials ("N" represents nylon; "P" represents polyester) and different pore sizes. Inset: comparison of SBP (5–8 cycles under stable algal growth) for the polyester MM with two pore sizes, 0.11 and 0.53 mm.

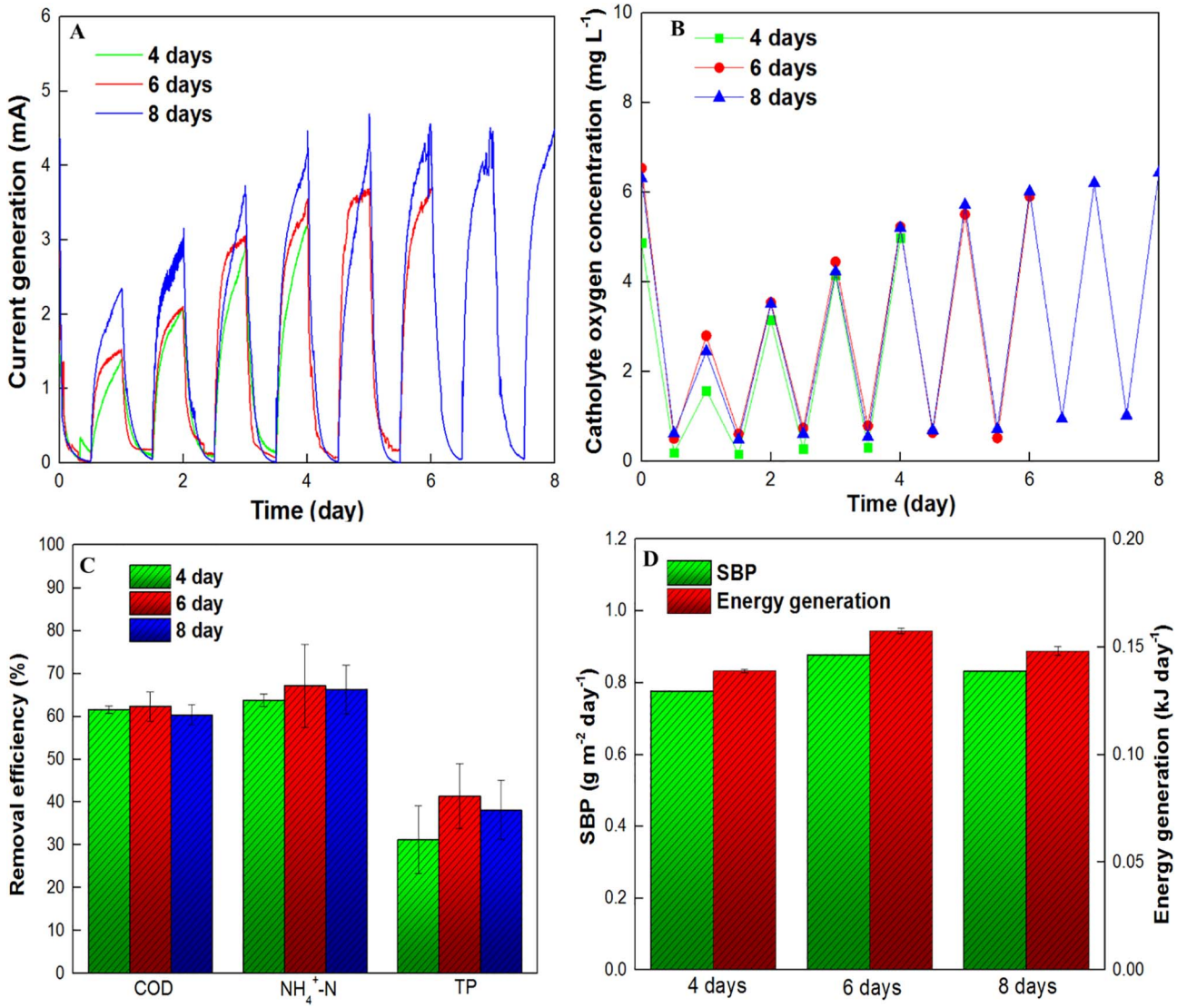

Fig. 3. The IPB performance affected by the algal growth/harvesting periods, 4, 6 and 8 days (Group 1): A) current profile; B) catholyte oxygen concentration; C) removal efficiency of COD, NH_4^+-N and TP; and D) SBP and daily energy generation (kJ day^{-1}).

efficiencies of COD, NH_4^+-N, and TP (Fig. 3C). The COD removal efficiency was 61.6 ± 0.83%, 62.3 ± 3.42%, and 60.4 ± 2.38%, for the growth/harvesting period of 4, 6, and 8 days, respectively ($p < .05$). In general, the IPB could remove 60–70% of NH_4^+-N and 25–40% of TP under all algal growth/harvesting periods.

The IPB operated under the algal growth/harvesting period of 6 days had a SBP of 0.88 g m^{-2} day^{-1}, greater than 0.78 and 0.83 g m^{-2} day^{-1} of 4 and 8 days, respectively (Fig. 3D). The lower productivity of the 8-day growth/harvesting period was possibly because that the formation of thick algal biofilm might have inhibited the light penetration and the transfer of carbon dioxide from the air for algal growth (Gross et al., 2013). In addition, the sloughing effect against the algal growth might be another reason to inhibit the algal growth with a longer growth/harvesting period (Gross and Wen, 2014). For the shorter growth/harvesting period of 4 days, frequent harvesting would keep the algal growth constantly at a lag phase, with a limited time for the acclimatization and growth before harvesting (Gross et al., 2013). Thus, the optimized algal growth period would be at 6 days in the present study. An appropriate algal growth/harvesting period could also improve energy generation, which included both electricity and algal biomass. The energy generation of the 6-day growth/harvesting period was 0.157 ± 0.001 kJ day^{-1}, statistically higher than 0.148 ± 0.002 kJ day^{-1} of 8 days ($p < .05$, Fig. 3D), and the major difference in energy generation was due to different algal biomass production. More algal biomass with the 6-day growth/harvesting period also benefited from its higher harvesting efficiency of 58.4% (Supplementary Fig. S4). The lower harvesting efficiency of the 8-day growth/harvesting period (53.1%) was possibly attributed to the cell shading and sloughing effect due to stronger susceptibility with thicker algal biofilm, and thus re-grown algae was easily to be washed off MM under a turbulent condition (Boelee et al., 2011; Gross and Wen, 2014). In summary, an algal growth/harvesting period of 6 days was determined to be optimal and used in the following experiments.

3.3. Effects of harvesting frequency in a cycle (Group 2)

Because of the benefit of residue algal biomass to continuing growth (for next harvesting cycle), it would be of interest to investigate whether the biomass should be collected completely at one time or partially with multiple collections within a cycle. To do this, three tests were performed with one, two, and three pieces of MM, each of them had the same total surface area, and each test had the same total growth/harvesting period of 6 days. It meant that in the case two pieces of MM, each would be removed for algal biomass harvesting every three days,

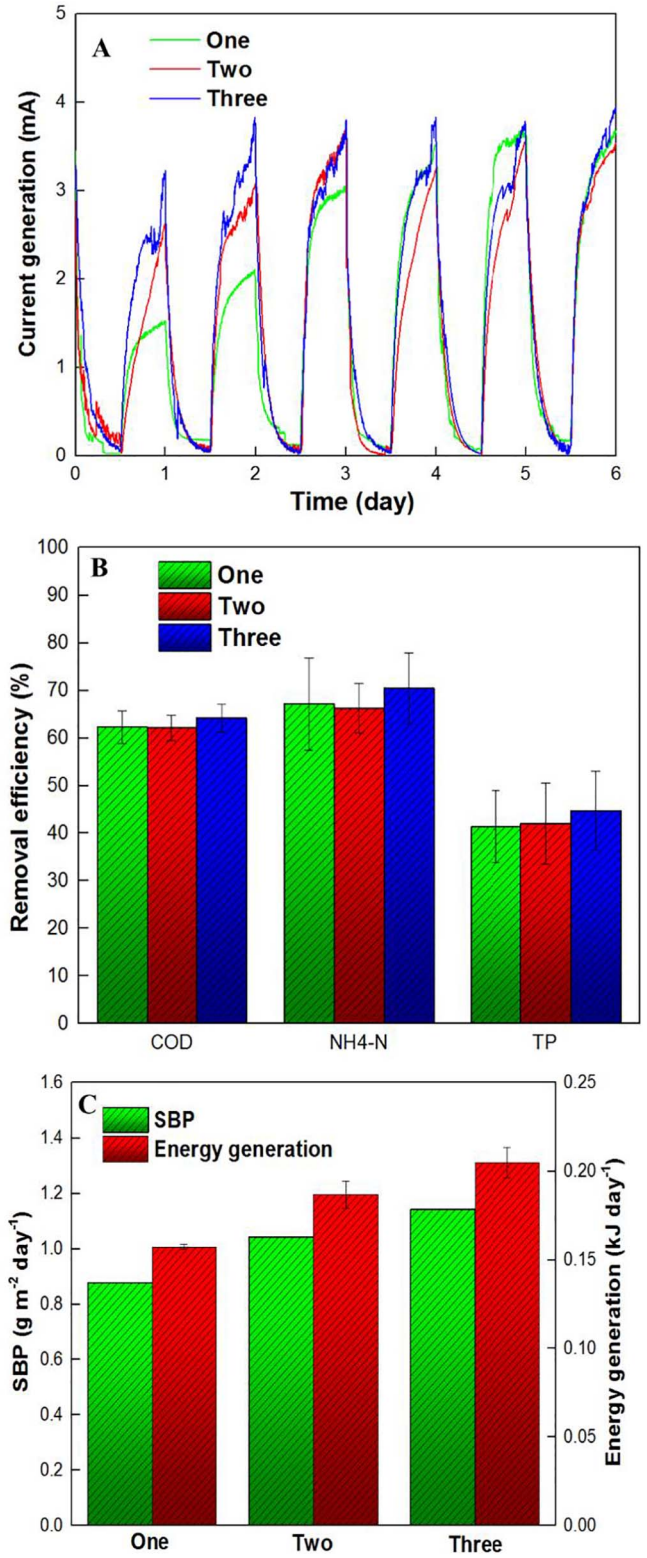

Fig. 4. The IPB performance affected by harvesting frequency: (Group 2): A) current generation; B) removal efficiency of COD, NH_4^+-N and TP; and C) SBP and daily energy generation. Note: "one, two, three" represent three tests in this group that contained different number of MM pieces with the same total surface area in each test.

and in the case of three pieces of MM, each would be harvested every two days (Supplementary Table S2). The peak current generations at the end of one cycle for the harvesting frequencies at 1, 2 and 3 time/cycle days were similar in the range of 3.5–3.7 mA, indicating the limited impact of changing harvesting frequencies on the current generation and the DO supply was sufficient under all three conditions (Fig. 4A). The total Coulomb production of three tests were not significantly different, at 141.3 ± 13.4 C day^{-1}, 124.9 ± 27.2 C day^{-1} and 121.3 ± 37.0 C day^{-1} with the harvesting frequencies at 2, 3, and 1 time/cycle days, respectively ($p > .05$). In addition, the IPB did not behave differently in terms of the organic and nutrient removal for all harvesting frequencies, and achieved the removal efficiency of about 60–65%, 60–70% and 30–50% for COD, NH_4^+-N, and TP, respectively ($p > .05$, Fig. 4B).

It was found that partial harvesting (multiple collections in a cycle) could improve algal biomass production and thus energy generation. The SBP of the third test (with three pieces of MM) was the highest at 1.14 g m^{-2} day^{-1}, compared to that of the one-piece MM test (0.88 m^{-2} day^{-1}) and the two-piece MM test (1.04 g m^{-2} day^{-1}) (Fig. 4C), while the algal harvesting efficiency was comparable among the three tests (Supplementary Fig. S5). This high SBP in the third test resulted in the highest energy generation of 0.205 ± 0.009 kJ day^{-1} ($p < .05$, Fig. 4C). However, more frequent harvesting would also lead to more algal loss. The total amount of the uncollected algal biomass in the third test was 0.0201 g day^{-1}, greater than that of the one-piece MM test (0.0163 g day^{-1}) and two-piece MM test (0.0180 g day^{-1}) (Supplementary Fig. S5). In general, algal harvesting based on the three-piece MM approach could benefit algal growth and collection and was used in the following experiments.

3.4. Effects of the catholyte mixing method (Group 3)

Catholyte mixing is critically important to provide sufficient mass transfer of both DO (to the cathode for reduction reaction) and nutrients (to algae for growth). However, the use of stirring to provide mixing is not practical. In a treatment system, mixing is usually provided by either mechanical agitation, aeration, or hydraulic recirculation. In this experiment, hydraulic recirculation was employed by recirculating the catholyte; for comparison, constant aeration of air in the absence of algae was also conducted (Group 3, Supplementary Table S2).

The current generation of three operational conditions was shown in Fig. 5A. The system with constant aeration exhibited average current output of 3.22 mA and the average current density based on the anode volume was 8.05 A m^{-3}. For the IPB system, the use of algae to provide DO resulted in day/night variation affected by photosynthesis, and thus the average current densities (including current generation at night) under the stirring and the catholyte recirculation conditions were only 4.93 A m^{-3} and 5.11 A m^{-3} (anode volume) during 5–8 cycles, respectively. The total Coulomb production and the Coulombic efficiency with the aeration was 276.6 ± 1.3 C day^{-1} and 20.9 ± 0.6%, much higher than those by either the stirring (169.4 ± 39.9 C day^{-1} and 12.1 ± 2.5%) or the catholyte recirculation (176.0 ± 21.8 C day^{-1} and 12.6 ± 1.3%) ($p < .05$). Such difference was due to DO supply, which influences cathodic oxygen reduction reaction and thus the current generation. The IPB performance of COD and NH_4^+-N removal was comparable to that with constant aeration (Fig. 5B, $p > .05$). However, the treatment efficiency of TN and TP was significant enhanced in the presence of algae, at 46.04 ± 3.15% (TN) and 43.95 ± 4.53% (TP) with the stirring, or 37.53 ± 5.14% (TN) and 42.36 ± 2.69% (TP) with the catholyte recirculation, higher than 25.33 ± 2.91% (TN) and 7.41 ± 5.69% (TP) with constant aeration ($p < .05$). The introduction of algae for their attachment on the mesh membrane would also bring various bacterial species into the IPB cathode (in both solution and cathodic biofilm), especially after a long-term operation (Ma et al., 2014). In addition, the oxygen concentration difference between the daytime and night, and the oxygen gradient between cathodic biofilm and the solution would colonize different anaerobic and aerobic microorganisms with various metabolic pathways, some of which could improve the nutrient removal, such as nitrification and denitrification (Rago et al., 2017). Thus, the higher TN

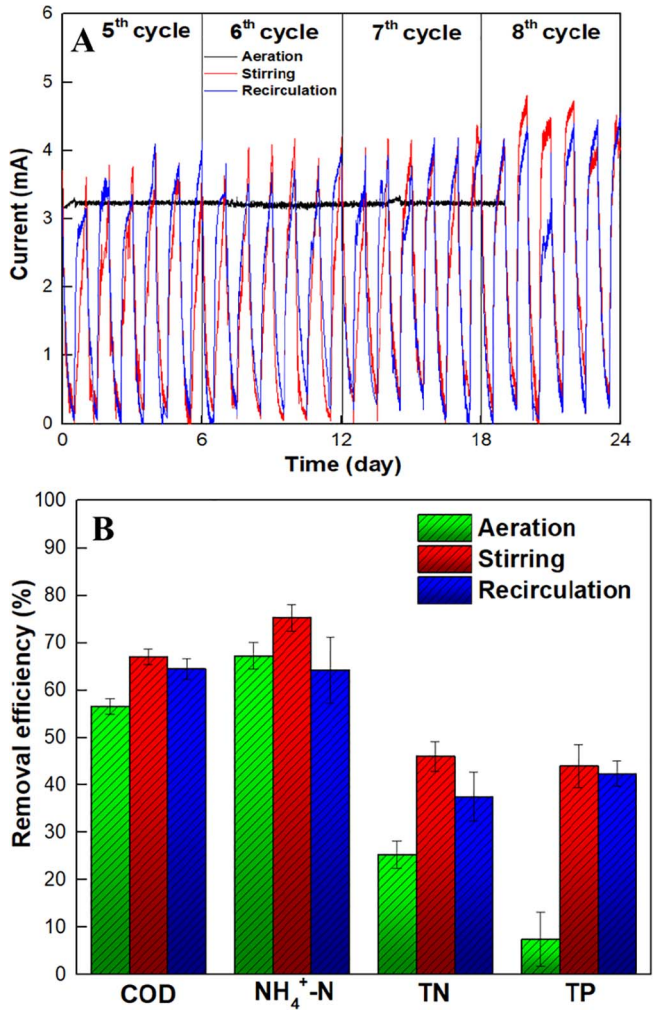

Fig. 5. The IPB performance under three catholyte mixing/DO supply conditions (Group 3): A) current generation; B) removal efficiency of COD, NH_4^+-N, TN (including NH_4^+-N and NO_3^--N) and TP.

and TP removal rates in the IPB have demonstrated the importance of algae in nutrient removal in the proposed system.

The SBP trend was similar to the trend of the cathodic oxygen concentration for both operating conditions (Fig. 6A and B; note: the aeration-system did not have algal growth), but the IPB with the stirring produced a lightly higher SBP of 1.62 ± 0.06 $g\,m^{-2}\,day^{-1}$ than that using the catholyte recirculation (1.46 ± 0.06 $g\,m^{-2}\,day^{-1}$, $p < .05$), based on the algal harvesting in 5–8 cycles (Fig. 6A), likely related to the flushing effect of the catholyte recirculation that could wash off the algae from the MM. This washing-off effect could also be the reason of a lower cathodic oxygen concentration in the early stage of the operation (1–4 cycles with slower algal biofilm development) under the condition of the catholyte recirculation; eventually, both conditions had similar cathodic oxygen concentrations (6.05 ± 0.78 $mg\,L^{-1}$ with the catholyte recirculation vs. 6.41 ± 0.31 $mg\,L^{-1}$ with the stirring, Fig. 6B, $p > .05$). The methods to further improve SBP warrant future investigation, such as the optimization of the bicarbonate concentration in the cathode because of its influence on the photosynthetic process and the oxygen concentration (Kakarla et al., 2015). In addition, the HRT of the catholyte may also affect SBP. Compared with the prior IPB systems that have the tubular MFCs and continuous operation of the anode effluent to the cathode (Supplementary Table S3), the algal productivity (normalized to per volume of treated wastewater) of the present IPB was much higher at 72.3 $g\,m^{-3}$ (treated wastewater), indicating the effectiveness of the MM-based harvesting method.

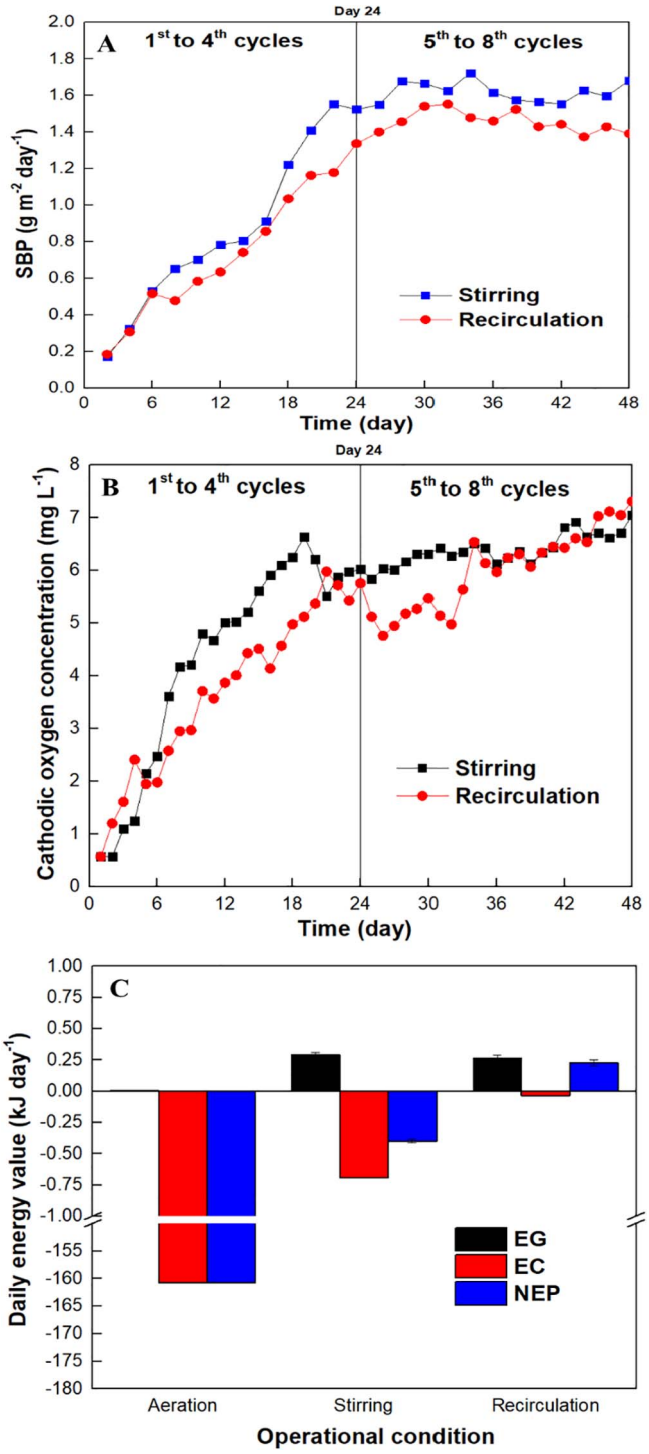

Fig. 6. The energy performance of the IPB system under three catholyte mixing/DO supply conditions: A) SBP ($g\,m^{-2}\,day^{-1}$) under the conditions of stirring and catholyte recirculation; B) cathodic oxygen concentration under the conditions of stirring and catholyte recirculation; and C) energy generation (EG), consumption (EC), and net energy production (NEP) under three conditions (data from the 5th to 8th cycles).

The energy performance of three catholyte mixing conditions from the relatively stable period (last 4 cycles) was shown in Fig. 6C. Despite higher total Coulomb production, the aerated MFC had energy generation of only 0.004 ± 0.001 $kJ\,day^{-1}$, much lower than that under the stirring condition (0.292 ± 0.017 $kJ\,day^{-1}$) or the catholyte recirculation (0.263 ± 0.025 $kJ\,day^{-1}$), because of the lack of algal biomass production. In addition, the energy consumption of the aerated MFC was −160.7 $kJ\,day^{-1}$, several orders of magnitudes higher than

that the IPB system under the stirring condition ($-0.691\,kJ\,day^{-1}$) or the catholyte recirculation ($-0.036\,kJ\,day^{-1}$). As a result, the aerated MFC had the most negative NEP of $-160.695 \pm 0.001\,kJ\,day^{-1}$ (or the largest net energy demand). For the IPB system under two catholyte mixing conditions, the catholyte recirculation resulted in a positive NEP of $0.227 \pm 0.025\,kJ\,day^{-1}$, while the stirring still led to a negative NEP of $-0.411 \pm 0.023\,kJ\,day^{-1}$ due to its higher energy consumption than production. Therefore, the catholyte recirculation was proved to be an effective mixing method with the best overall energy performance.

4. Conclusions

This study has demonstrated a new method for algal collection based on mesh membrane in a newly designed IPB system that had algal growth physically separated from the cathode electrode to facilitate harvesting. Both MM material and pore size were experimentally determined for optimal algal growth. The key factors such as algal growth/harvesting period and harvesting frequency were examined. It was shown that the catholyte recirculation was an effective approach for catholyte mixing with a theoretically positive energy output from the IPB. Those results would encourage further efforts of developing IPB systems for sustainable bioenergy recovery from wastewater treatment.

Acknowledgements

This work was financially supported by a National Science Foundation award 1603190 and a 4 VA research grant from Virginia Tech.

Appendix A. Supplementary data

Supplementary data associated with this article can be found, in the online version, at http://dx.doi.org/10.1016/j.biortech.2018.01.001.

References

Boelee, N.C., Temmink, H., Janssen, M., Buisman, C.J., Wijffels, R.H., 2011. Nitrogen and phosphorus removal from municipal wastewater effluent using microalgal biofilms. Water Res. 45 (18), 5925–5933.

Christenson, L.B., Sims, R.C., 2012. Rotating algal biofilm reactor and spool harvester for wastewater treatment with biofuels by-products. Biotechnol. Bioeng. 109 (7), 1674–1684.

Demirbas, A., Fatih Demirbas, M., 2011. Importance of algae oil as a source of biodiesel. Energy Convers. Manage. 52 (1), 163–170.

Escapa, A., San-Martín, M.I., Morán, A., 2014. Potential use of microbial electrolysis cells in domestic wastewater treatment plants for energy recovery. Front. Energy Res. 2, 19.

Gill, N., Appleton, M., Baganz, F., Lye, G., 2008. Quantification of power consumption and oxygen transfer characteristics of a stirred miniature bioreactor for predictive fermentation scale-up. Biotechnol. Bioeng. 100 (6), 1144–1155.

Gross, M., Henry, W., Michael, C., Wen, Z., 2013. Development of a rotating algal biofilm growth system for attached microalgae growth with in situ biomass harvest. Bioresour. Technol. 150, 195–201.

Gross, M., Jarboe, D., Wen, Z., 2015. Biofilm-based algal cultivation systems. Appl. Microbiol. Biotechnol. 99 (14), 5781–5789.

Gross, M., Wen, Z., 2014. Yearlong evaluation of performance and durability of a pilot-scale revolving algal biofilm (RAB) cultivation system. Bioresour Technol 171, 50–58.

Gross, M., Zhao, X., Mascarenhas, V., Wen, Z., 2016. Effects of the surface physico-chemical properties and the surface textures on the initial colonization and the attached growth in algal biofilm. Biotechnol. Biofuels 9, 38.

Henze, M., 2002. Wastewater Treatment: Biological and Chemical Processes. Springer Science & Business Media.

Hou, Q., Pei, H., Hu, W., Jiang, L., Yu, Z., 2016. Mutual facilitations of food waste treatment, microbial fuel cell bioelectricity generation and Chlorella vulgaris lipid production. Bioresour. Technol. 203, 50–55.

Kakarla, R., Kim, J.R., Jeon, B.-H., Min, B., 2015. Enhanced performance of an air–-cathode microbial fuel cell with oxygen supply from an externally connected algal bioreactor. Bioresour. Technol. 195, 210–216.

Kakarla, R., Min, B., 2014. Evaluation of microbial fuel cell operation using algae as an oxygen supplier: carbon paper cathode vs. carbon brush cathode. *Bioprocess*. Biosyst. Eng. 37 (12), 2453–2461.

Kesaano, M., Sims, R.C., 2014. Algal biofilm based technology for wastewater treatment. Algal Res. 5, 231–240.

Liu, T., Wang, J., Hu, Q., Cheng, P., Ji, B., Liu, J., Chen, Y., Zhang, W., Chen, X., Chen, L., Gao, L., Ji, C., Wang, H., 2013. Attached cultivation technology of microalgae for efficient biomass feedstock production. Bioresour. Technol. 127, 216–222.

Logan, B.E., Hamelers, B., Rozendal, R., Schröder, U., Keller, J., Freguia, S., Aelterman, P., Verstraete, W., Rabaey, K., 2006. Microbial fuel cells: methodology and technology. Environ. Sci. Technol. 40 (17), 5181–5192.

Luo, S., Berges, J.A., He, Z., Young, E.B., 2017a. Algal-microbial community collaboration for energy recovery and nutrient remediation from wastewater in integrated photo-bioelectrochemical systems. Algal Res. 24, 527–539.

Luo, S., He, Z., 2016. Ni-coated carbon fiber as an alternative cathode electrode material to improve cost efficiency of microbial fuel cells. Electrochim. Acta 222, 338–346.

Luo, S., Wang, Z.-W., He, Z., 2017b. Mathematical modeling of the dynamic behavior of an integrated photo-bioelectrochemical system for simultaneous wastewater treatment and bioenergy recovery. Energy 124, 227–237.

Ma, J., Wang, Z., Zhang, J., Waite, T.D., Wu, Z., 2017. Cost-effective Chlorella biomass production from dilute wastewater using a novel photosynthetic microbial fuel cell (PMFC). Water Res. 108, 356–364.

Ma, X., Zhou, W., Fu, Z., Cheng, Y., Min, M., Liu, Y., Zhang, Y., Chen, P., Ruan, R., 2014. Effect of wastewater-borne bacteria on algal growth and nutrients removal in wastewater-based algae cultivation system. Bioresour. Technol. 167, 8–13.

Mata, T.M., Martins, A.A., Caetano, N.S., 2010. Microalgae for biodiesel production and other applications: a review. Renewable Sustainable Energy Rev. 14 (1), 217–232.

McCarty, P.L., Bae, J., Kim, J., 2011. Domestic wastewater treatment as a net energy producer–can this be achieved? Environ. Sci. Technol. 45 (17), 7100–7106.

Ozkan, A., Berberoglu, H., 2013. Physico-chemical surface properties of microalgae. Colloids Surf. B. 287–293.

Qin, M., Liu, Y., Luo, S., Qiao, R., He, Z., 2017. Integrated experimental and modeling evaluation of energy consumption for ammonia recovery in bioelectrochemical systems. Chem. Eng. J. 327, 924–931.

Rago, L., Cristiani, P., Villa, F., Zecchin, S., Colombo, A., Cavalca, L., Schievano, A., 2017. Influences of dissolved oxygen concentration on biocathodic microbial communities in microbial fuel cells. Bioelectrochemistry 116, 39–51.

Shi, J., Podola, B., Melkonian, M., 2014. Application of a prototype-scale Twin-Layer photobioreactor for effective N and P removal from different process stages of municipal wastewater by immobilized microalgae. Bioresour. Technol. 154, 260–266.

Su, Y., Mennerich, A., Urban, B., 2016. The long-term effects of wall attached microalgal biofilm on algae-based wastewater treatment. Bioresour. Technol. 218, 1249–1252.

Tse, H.T., Luo, S., Li, J., He, Z., 2016. Coupling microbial fuel cells with a membrane photobioreactor for wastewater treatment and bioenergy production. Bioprocess Biosyst. Eng. 39 (11), 1703–1710.

Wang, H., Park, J.D., Ren, Z.J., 2015. Practical energy harvesting for microbial fuel cells: a review. Environ. Sci. Technol. 49 (6), 3267–3277.

Wei, Y., Van Houten, R.T., Borger, A.R., Eikelboom, D.H., Fan, Y., 2003. Minimization of excess sludge production for biological wastewater treatment. Water Res. 37 (18), 4453–4467.

Xiao, L., He, Z., 2014. Applications and perspectives of phototrophic microorganisms for electricity generation from organic compounds in microbial fuel cells. Renewable Sustainable Energy Rev. 37, 550–559.

Xiao, L., Young, E.B., Berges, J.A., He, Z., 2012. Integrated photo-bioelectrochemical system for contaminants removal and bioenergy production. Environ. Sci. Technol. 46 (20), 11459–11466.

Zhang, D., Fung, K.Y., Ng, K.M., 2014. Novel filtration photobioreactor for efficient biomass production. Ind. Eng. Chem. Res. 53 (33), 12927–12934.

Zhang, F., Ge, Z., Grimaud, J., Hurst, J., He, Z., 2013. Improving electricity production in tubular microbial fuel cells through optimizing the anolyte flow with spiral spacers. Bioresour. Technol. 134, 251–256.

Zhang, Q., Liu, C., Li, Y., Yu, Z., Chen, Z., Ye, T., Wang, X., Hu, Z., Liu, S., Xiao, B., Jin, S., 2017. Cultivation of algal biofilm using different lignocellulosic materials as carriers. Biotechnol. Biofuels. 10, 115.